Research on Quasi-isotropic Radiation of Small Circular Arc Antenna

Hailong Liu[1], Jinbo Liu[1], Xiaoxia Nie[1], Jiming Song[2], and Zengrui Li[1]

[1]School of Information and Communication Engineering
Communication University of China, Beijing, 100024, China
liuhailong@cuc.edu.cn, liuj@cuc.edu.cn, nxiaoxia@cuc.edu.cn, zrli@cuc.edu.cn

[2]Department of Electrical and Computer Engineering
Iowa State University, Ames, IA 50011, USA
jisong@iastate.edu

***Abstract* –** The radiation characteristics of circular arc antennas are studied by applying the method of moments (MoM) to solve the electric field integral equation (EFIE). Based on the triangular current distribution of small circular arc antennas, the analytical expression of radiation fields of circular arc antennas is derived. It is found that the circular arc antenna is equivalent to a superposition of an electric dipole and a magnetic dipole, resulting in near isotropic radiation pattern. Finally, both MoM and CST simulations show that the small arc antenna can realize the near isotropic radiation pattern.

***Index Terms* –** Circular arc antenna, electric field integral equation (EFIE), method of moments (MoM), quasi-isotropic radiation.

I. INTRODUCTION

Isotropic antennas can radiate electromagnetic energy equally in all directions [1]. However, isotropic antennas are impossible in theory, because the transverse electric field in the far field region cannot be uniform over a sphere if the field is linearly polarized everywhere [2], [3]. So quasi-isotropic antennas were proposed and commonly used in applications such as radio frequency identification, radio frequency energy harvesting, and wireless access points [4].

Design approaches for quasi-isotropic antennas include folded dipoles [5], magnetic dipoles [6], orthogonal dipoles [2], combination of multiple dipoles [7], split ring resonators [8], and so on. This paper will introduce a new approach based on circular arc antennas.

An arc antenna is a usual deformation of a dipole antenna, which is the simplest and most basic of various antenna structures. Although the circular arc antenna is simple, it still has characteristics that are worth study for applications. For example, using a circular antenna in a logging tool as a receiving antenna has great advantages in ultra-deep boundary detection [9]. It is more convenient to analyze the circular arc antenna by applying the method of moments (MoM) to solve the electric field integral equation (EFIE) than the traditional analytical method [10]. In this paper, based on the conclusion that the small circular arc antenna can be equivalent to a superposition of an electric dipole and a magnetic dipole in [11], it is proposed that the small circular arc antenna can realize quasi-3D omnidirectional radiation. As a result, the arc antenna can be used to overcome the zero-reading problem of dipole antennas [12].

II. THEORY AND FORMULA DERIVATION

A. Derivation of circular arc antenna EFIE

The EFIE for the antennas or scatterers which are perfect electric conductor (PEC) can be expressed as [10]

$$\mathrm{j}\omega\mu_0\hat{t}\bullet\iint_S\left[\mathbf{J}_S(\mathbf{r}')+\tfrac{1}{k^2}\nabla'\bullet\mathbf{J}_S(\mathbf{r}')\nabla\right]g(\mathbf{r},\mathbf{r}')\,dS' = \hat{t}\bullet\mathbf{E}^i(\mathbf{r}), \tag{1}$$

where $\mathbf{J}_S$ is the induced surface current, g is the Green's function, k and μ_0 are the wave number and permeability of the free space, and $\hat{t}$ denotes any tangential unit vector to the PEC surface.

The geometry for the circular arc antenna of radius b and line radius a is depicted in Fig. 1. If $b << \lambda$, where λ is the wavelength, the antenna can be regarded as a

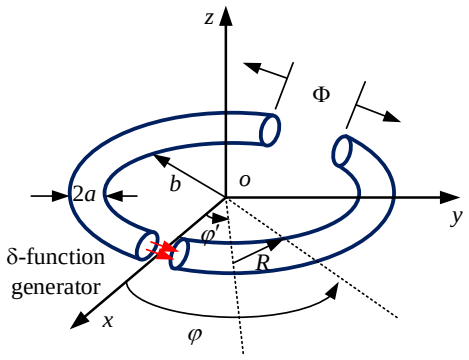

Fig. 1. Circular arc antenna geometry.

Submitted On: February 26, 2023
Accepted On: June 19, 2023

https://doi.org/10.13052/2023.ACES.J.380911

small circular arc antenna. And if $a << 2\pi b$, the antenna can be regarded as a thin wire antenna. Considering the thin wire antenna approximations, the source point $\mathbf{r}'$ and field point $\mathbf{r}$ can be represented by source point $\boldsymbol{\rho}'$ and field point $\boldsymbol{\rho}$. In addition,

$$\mathbf{J}_S(\mathbf{r}') = I(\varphi')\hat{\varphi}'/(2\pi a), \tag{2}$$

$$\hat{t} = \hat{\varphi}, \tag{3}$$

$$\hat{\varphi} \bullet \hat{\varphi}' = \cos(\varphi - \varphi'), \tag{4}$$

$$g(\varphi, \varphi') = \frac{e^{-\mathrm{j}kR}}{4\pi R}, \tag{5}$$

where R is the distance from the source point $\boldsymbol{\rho}'$ to the field point $\boldsymbol{\rho}$, expressed as

$$R = \sqrt{(a+b)^2 + b^2 - 2(a+b)b\cos(\varphi - \varphi')}$$
$$= \sqrt{a^2 + 4b(a+b)\sin^2[(\varphi - \varphi')/2]}. \tag{6}$$

By substituting (2)-(6) into (1), the EFIE suitable for the circular arc antenna is rewritten as

$$\int_{-\Phi/2}^{\Phi/2} I(\varphi') K(\varphi, \varphi') d\varphi' = -\mathrm{j}\frac{kb}{\eta} E_{\varphi}^{i}, \tag{7}$$

with

$$K(\varphi, \varphi') = \left[(kb)^2 \cos(\varphi - \varphi') + \frac{\partial^2}{\partial \varphi^2}\right] g(\varphi, \varphi'). \tag{8}$$

B. Radiation field and equivalent model of circular arc antenna

The relationship between magnetic potential A and current vector $\mathbf{I}(\mathbf{r}')$ of the circular arc antenna is

$$\mathbf{A} = \frac{\mu}{4\pi}\int_C \mathbf{I}(\mathbf{r}')\frac{e^{-\mathrm{j}kR}}{R} dl', \tag{9}$$

where $\mathbf{I}(\mathbf{r}') = I(\varphi')\hat{\varphi}'$ and $dl' = bd\varphi'$. Therefore, (9) can be changed to

$$\mathbf{A} = \frac{b\mu}{4\pi}\int_{-\Phi/2}^{\Phi/2} I(\varphi')\hat{\varphi}'\frac{e^{-\mathrm{j}kR}}{R} d\varphi'. \tag{10}$$

In the spherical coordinate system, $\mathbf{A}$ can be expressed by the sum of the components in r, θ, and φ directions, that is

$$\mathbf{A}(r, \theta, \varphi) = A_r(r, \theta, \varphi)\hat{r} + A_\theta(r, \theta, \varphi)\hat{\theta} + A_\varphi(r, \theta, \varphi)\hat{\varphi}. \tag{11}$$

The vector potential is expressed as [13]

$$\begin{cases} A_r = \frac{b\mu_0}{4\pi}\sin\theta\int_{-\Phi/2}^{\Phi/2} I(\varphi')\sin(\varphi - \varphi')\frac{e^{-\mathrm{j}kR}}{R} d\varphi' \\ A_\theta = \frac{b\mu_0}{4\pi}\cos\theta\int_{-\Phi/2}^{\Phi/2} I(\varphi')\sin(\varphi - \varphi')\frac{e^{-\mathrm{j}kR}}{R} d\varphi' \\ A_\varphi = \frac{b\mu_0}{4\pi}\int_{-\Phi/2}^{\Phi/2} I(\varphi')\cos(\varphi - \varphi')\frac{e^{-\mathrm{j}kR}}{R} d\varphi' \end{cases}. \tag{12}$$

According to the far field approximation [14], $R \approx r - b\sin\theta\cos(\varphi - \varphi')$, the magnetic potential $\mathbf{A}$ is then transformed into

$$\begin{cases} A_r = \frac{b\mu_0 e^{-\mathrm{j}kr}}{4\pi r}\sin\theta\int_{-\Phi/2}^{\Phi/2} I(\varphi')\sin(\varphi - \varphi')e^{\mathrm{j}kb\sin\theta\cos(\varphi - \varphi')} d\varphi' \\ A_\theta = \frac{b\mu_0 e^{-\mathrm{j}kr}}{4\pi r}\cos\theta\int_{-\Phi/2}^{\Phi/2} I(\varphi')\sin(\varphi - \varphi')e^{\mathrm{j}kb\sin\theta\cos(\varphi - \varphi')} d\varphi' \\ A_\varphi = \frac{b\mu_0 e^{-\mathrm{j}kr}}{4\pi r}\int_{-\Phi/2}^{\Phi/2} I(\varphi')\cos(\varphi - \varphi')e^{\mathrm{j}kb\sin\theta\cos(\varphi - \varphi')} d\varphi' \end{cases}. \tag{13}$$

For a small circular arc antenna, the current distribution obtained by the MoM is shown in Fig. 2. Obviously,

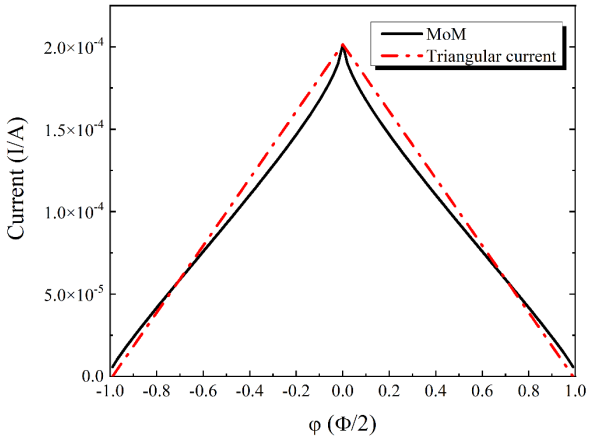

Fig. 2. Circular arc antenna current when $kb = 2\pi\times10^{-4}$.

the current distribution is close to the triangular current and can be written as

$$I(\varphi') = I_A(1 - 2|\varphi'|/\Phi) \quad -\Phi/2 \le \varphi' \le \Phi/2, \tag{14}$$

where I_A is the peak value of current amplitude calculated with MoM.

With small arc approximation, $e^{\mathrm{j}kb\sin\theta\cos(\varphi - \varphi')}$ can be expanded to $1 + \mathrm{j}kb\sin\theta\cos(\varphi - \varphi')$. Substituting (14) into (13) as well as integrating them respectively yields

$$\begin{cases} A_r = \frac{b\mu_0 e^{-\mathrm{j}kr}\sin\theta I_A}{4\pi r\Phi}\left[\begin{array}{l} 8\sin\varphi\sin^2(\Phi/4) \\ +\mathrm{j}kb\sin\theta\sin(2\varphi)\sin^2(\Phi/2)\end{array}\right] \\ A_\theta = \frac{b\mu_0 e^{-\mathrm{j}kr} I_A}{8\pi r\Phi}\left[\begin{array}{l} 16\cos\theta\sin\varphi\sin^2(\Phi/4) \\ +\mathrm{j}kb\sin(2\theta)\sin(2\varphi)\sin^2(\Phi/2)\end{array}\right] \\ A_\varphi = \frac{b\mu_0 e^{-\mathrm{j}kr} I_A}{16\pi r\Phi}\left\{\begin{array}{l} 32\cos\varphi\sin^2(\Phi/4) \\ +\mathrm{j}kb\sin\theta\left[\Phi^2 + 4\cos(2\varphi)\sin^2(\Phi/2)\right]\end{array}\right\} \end{cases}. \tag{15}$$

In the spherical coordinate system, the expression of electric field $\mathbf{E}^S$ in far field region is

$$\mathbf{E}^S = -\mathrm{j}\omega\left(\hat{\theta}A_\theta + \hat{\varphi}A_\varphi\right) \tag{16}$$

with

$$\begin{cases} E_\theta = \frac{-\mathrm{j}\omega b\mu_0 e^{-\mathrm{j}kr} I_A}{8\pi r\Phi}\left[\begin{array}{l} 16\cos\theta\sin\varphi\sin^2(\Phi/4) \\ +\mathrm{j}kb\sin(2\theta)\sin(2\varphi)\sin^2(\Phi/2)\end{array}\right] \\ E_\varphi = \frac{-\mathrm{j}\omega b\mu_0 e^{-\mathrm{j}kr} I_A}{16\pi r\Phi}\left\{\begin{array}{l} 32\cos\varphi\sin^2(\Phi/4) + \mathrm{j}kb\sin\theta \\ \left[\Phi^2 + 4\cos(2\varphi)\sin^2(\Phi/2)\right]\end{array}\right\} \end{cases}. \tag{17}$$

The small circular arc antenna can be characterized by an electric dipole moment $I_e l$ and a magnetic dipole moment $I_m l$ [15]. Next, we will discuss the radiation field expressions of the electric dipole and magnetic dipole.

The position of the electric dipole along the y-direction located at $x = x_e$ along x-axis is shown in Fig. 3 (a). Then, the magnetic vector potential $\mathbf{A}$ is

$$\mathbf{A}(\mathbf{r}) = \hat{y}\frac{\mu I_e l}{4\pi}\frac{e^{-\mathrm{j}kR}}{R}, \tag{18}$$

where

$$R = \sqrt{r^2 - 2x_e r\sin\theta\cos\varphi + x_e^2}. \tag{19}$$

Considering $r >> x_e$, R can be written as

$$R = r\sqrt{1 - 2\frac{x_e}{r}\sin\theta\cos\varphi + \left(\frac{x_e}{r}\right)^2} \approx r - x_e\sin\theta\cos\varphi, \quad (20)$$

thus,

$$\frac{e^{-\mathrm{j}kR}}{R} \approx \frac{e^{-\mathrm{j}k(r - x_e\sin\theta\cos\varphi)}}{r}. \quad (21)$$

Therefore, (18) can be simplified as

$$\mathbf{A}(\mathbf{r}) = \hat{y}\frac{\mu I_e l}{4\pi r}e^{-\mathrm{j}k(r - x_e\sin\theta\cos\varphi)}, \quad (22)$$

where $\hat{y} = \hat{r}\sin\theta\sin\varphi + \hat{\theta}\cos\theta\sin\varphi + \hat{\varphi}\cos\varphi$.

The radiation field expressions of the electric dipole along the y-direction located at $x = x_e$ are then

$$\begin{cases} E_\theta^e = -\mathrm{j}\eta\frac{kI_e l\cos\theta\sin\varphi}{4\pi r}e^{-\mathrm{j}k(r - x_e\sin\theta\cos\varphi)} \\ E_\varphi^e = -\mathrm{j}\eta\frac{kI_e l\cos\varphi}{4\pi r}e^{-\mathrm{j}k(r - x_e\sin\theta\cos\varphi)} \end{cases}. \quad (23)$$

The position of the magnetic dipole along the z-direction located at $x = x_m$ along the x-axis is shown in Fig. 3 (b). Its radiation field expression that can be derived in the same way is

$$\begin{cases} E_\theta^m = 0 \\ E_\varphi^m = -\frac{\mathrm{j}kI_m l\sin\theta}{4\pi r}e^{-\mathrm{j}k(r - x_m\sin\theta\cos\varphi)} \end{cases}. \quad (24)$$

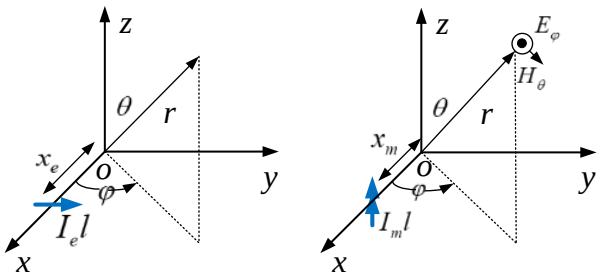

(a) (b)

Fig. 3. Schematic diagrams of (a) an electric dipole and (b) a magnetic dipole.

By comparing the radiation field expression (17) with (23) and (24), it is concluded that the small circular arc antenna can be equivalent to a superposition of an electric dipole along the y direction located at $x_e = b\cos^2(\Phi/4)$ and a magnetic dipole along z direction located at $x_m = x_e$ as shown in Fig. 4.

The electric dipole moment is expressed as

$$I_e l = \left[8bI_A\sin^2(\Phi/4)\right]/\Phi, \quad (25)$$

and the magnetic moment is given as

$$I_m l = \frac{\mathrm{j}\omega\mu I_A b^2\Phi}{4}\left[1 - \frac{4\sin^2(\Phi/2)}{\Phi^2}\right]. \quad (26)$$

For a very small arc antenna with $\Phi << 1$, we have

$$x_e = x_m = b,\ I_e l = \frac{I_A b}{2}\Phi,\ I_m l = \frac{\mathrm{j}\omega\mu I_A b^2}{12}\Phi^3 \to 0. \quad (27)$$

For one half circular arc antenna with $\Phi = \pi$,

$$x_e = x_m = \frac{b}{2},\ I_e l = \frac{4I_A b}{\pi},\ I_m l = \frac{\mathrm{j}\omega\mu I_A\pi b^2}{4}\left(1 - \frac{4}{\pi^2}\right). \quad (28)$$

Similarly, for a full loop with a gap,

$$x_e = x_m = 0,\ I_e l = \frac{4I_A b}{\pi},\ I_m l = \frac{\mathrm{j}\omega\mu I_A\pi b^2}{2}. \quad (29)$$

For a full loop without a gap, we have the well-known results [16]

$$x_e = x_m = 0,\ I_e l = 0,\ I_m l = \mathrm{j}\omega\mu I_A\pi b^2. \quad (30)$$

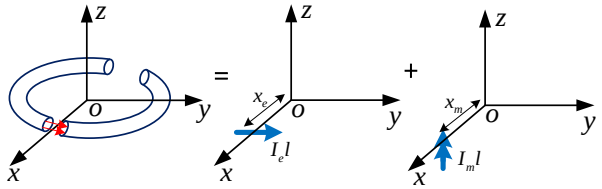

(a) (b) (c)

Fig. 4. Equivalent model of a circular arc antenna: (a) Circular arc antenna with angle Φ, (b) electric dipole $I_e l$, and (c) magnetic dipole $I_m l$.

C. Electric dipole and magnetic dipole

The normalized pattern of an antenna is defined as

$$F(\theta,\varphi) = \frac{|E(\theta,\varphi)|}{E_{\max}}. \quad (31)$$

According to the radiation field expressions (23) and (24), the normalized pattern of an electric dipole and a magnetic dipole are

$$\begin{cases} F_\theta^e = \cos\theta\sin\varphi \\ F_\varphi^e = \cos\varphi \end{cases}, \quad (32)$$

and

$$\begin{cases} F_\theta^m = \sin\theta \\ F_\varphi^m = 0 \end{cases}, \quad (33)$$

respectively, while their radiation patterns are shown in Fig. 5.

From the patterns of the electric dipole and magnetic dipole, their radiation intensity near the central axis is very low or even zero, but these axes are not the same. If the electric dipole and magnetic dipole are superimposed, the combined patterns can be complementary and will have no direction where the normalized pattern is zero.

Where the ratio of the electric dipole to magnetic dipole $I_e l/I_m l = n_e/\eta\ (0 < n_e < \infty)$ and where n_e is the normalized ratio, the electric field obtained by superposition of the electric dipole and magnetic dipole is

$$\begin{cases} E_\theta = n_e E_\theta^e + E_\theta^m \\ E_\varphi = n_e E_\varphi^e + E_\varphi^m \end{cases}. \quad (34)$$

According to equation (31), the normalized pattern of the superposition of an electric dipole and a magnetic dipole can be obtained, and the minimum can be found.

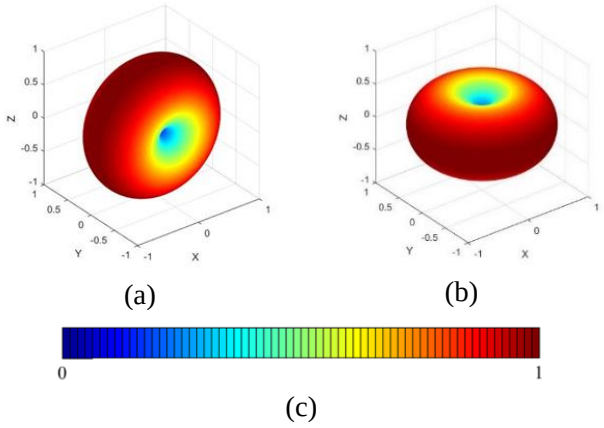

Fig. 5. Radiation patterns of (a) an electric dipole along the y direction and (b) a magnetic dipole along the z direction; (c) the color map.

III. NUMERICAL RESULTS AND ANALYSIS

The minimum value of the normalized pattern as a function of n_e is shown in Fig. 6. When n_e = 1, that is, $I_e l/I_m l = 1/\eta$, the minimum is $\sqrt{2}/2$, which is the largest, and the pattern is the closest to 3D omnidirectional, as shown in Fig. 7.

In Section II A, it is concluded that the small arc antenna can be equivalent to the superposition of an electric dipole and a magnetic dipole. In Section II B, it is shown that the superposition of an electric dipole and magnetic dipole can realize quasi-isotropic radiation. Therefore, it is predictable that the small arc antenna can realize quasi-isotropic radiation.

In order to obtain the gain deviation, namely, the difference between the maximum gain and the minimum

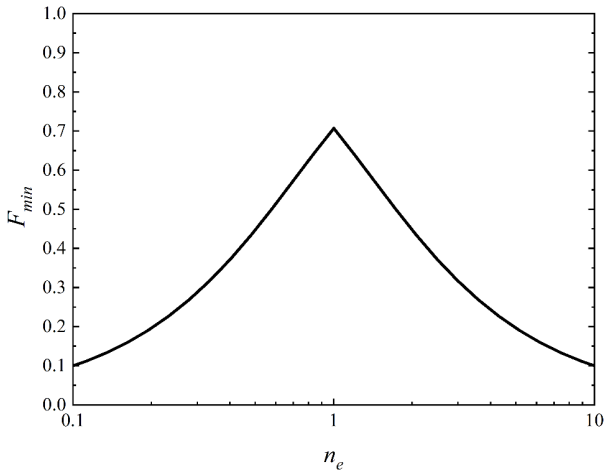

Fig. 6. Minimum value of normalized pattern of superposition of an electric dipole and a magnetic dipole.

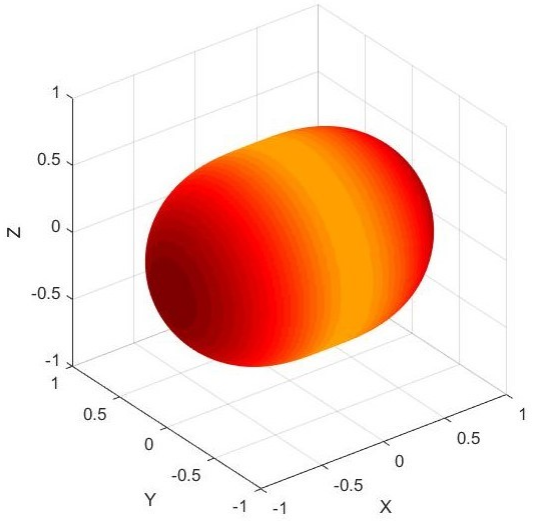

Fig. 7. When $I_e l/I_m l = 1/\eta$, the radiation pattern of the superposition of an electric dipole and a magnetic dipole. The color map is the same as that in Fig. 5 (c).

gain, and the radius of the arc when the pattern of the arc antenna with different angles Φ is the closest to 3D omni-directional, the MoM and the electromagnetic simulation software CST [17] are used to build the simulation model. The line radius of the arc is λ/1000 in both methods.

The gain deviation, radius, and arc length calculated by the two methods are compared and verified. Figure 8 shows the relationship between gain deviation and arc antenna angle. The difference in results between MoM and CST may be due to inconsistent meshing. In

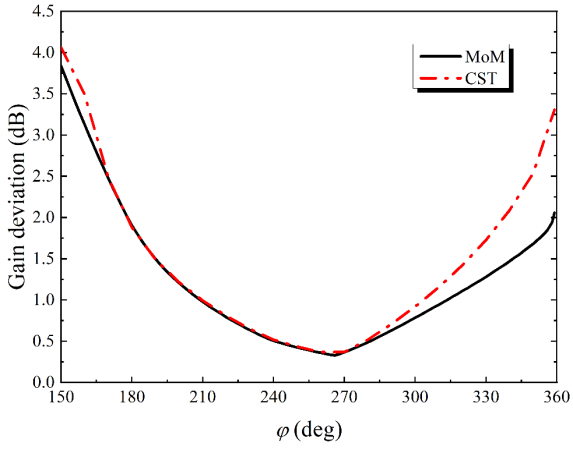

Fig. 8. Gain deviation of circular arc antenna with different angles when the arc antenna is the closest to 3D omnidirectional radiation.

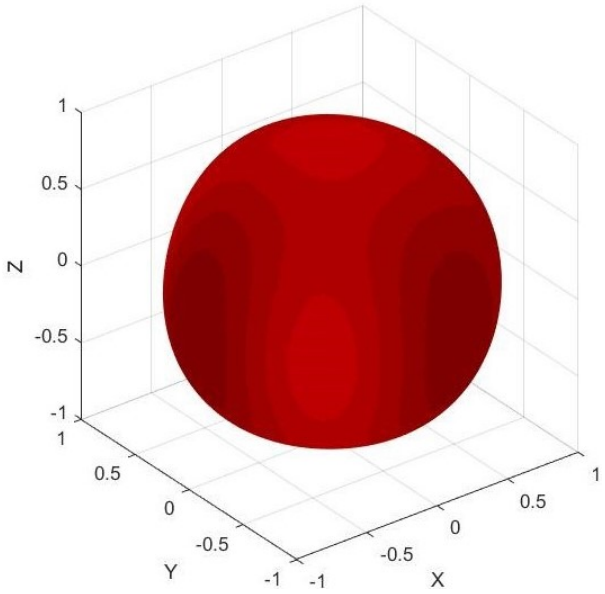

Fig. 9. The radiation pattern of 266-degree arc antenna which is the closest to isotropic radiation. The radius is 0.1542 λ. The color map is the same as that in Fig. 5 (c).

the results calculated by the MoM, the 266-degree arc antenna is the closest to 3D omnidirectional radiation, and the gain deviation is only 0.33 dB. The radiation pattern of the 266-degree arc antenna is shown in Fig. 9.

Figures 10 and 11 show the relationship between arc radius and arc antenna angle, and the relationship between arc length and arc antenna angle when the arc antenna is the closest to 3D omnidirectional radiation. It can be found that the arc radius and arc length decrease monotonically with the increase of the arc antenna angle.

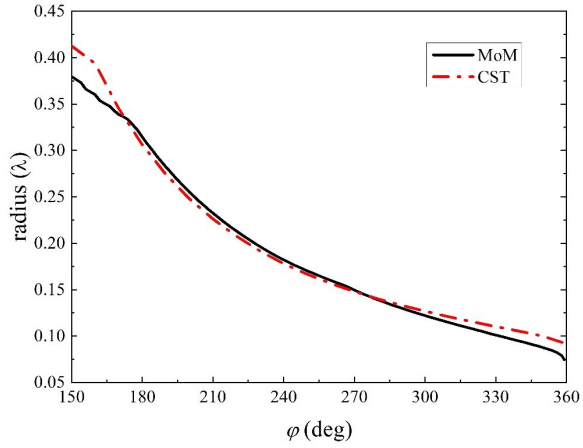

Fig. 10. Radius of circular arc antenna with different angles when the arc antenna is the closest to 3D omnidirectional radiation.

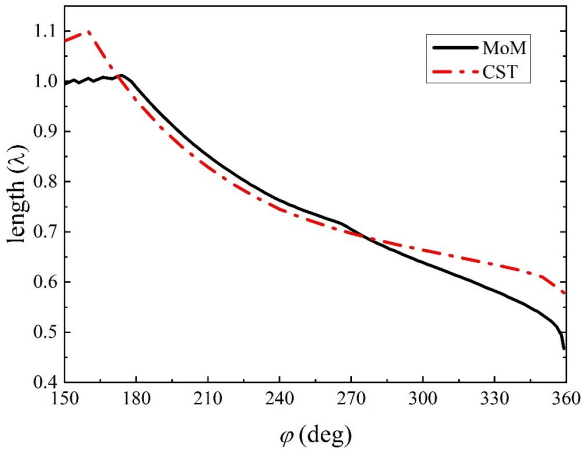

Fig. 11. Length of circular arc antenna with different angles when the arc antenna is the closest to near isotropic radiation.

That is to say, under this condition, when the arc is closer to a complete circle, the size is smaller. Although there are some differences in the simulation results of the two methods, the overall trend of change is consistent.

IV. SUMMARY

In this paper, the MoM is used to analyze the circular arc antenna. Firstly, the EFIE of the circular arc antenna is derived and verified by the known results of loop antennas. Secondly, the analytical approximate expression of the radiation field of the small circular arc antenna is derived by using the triangular current distribution. And by comparing the radiation field of circular arc antenna with that of electric dipole and magnetic dipole, it is concluded that the small circular arc antenna can be equivalent to a superposition of an electric dipole and a magnetic dipole. Thirdly, it is found that the superposition of an electric dipole and a magnetic dipole can realize quasi-3D omnidirectional radiation. Finally, by using MoM and CST software, it is shown that the small arc antenna can realize near isotropic radiation.

ACKNOWLEDGMENT

This work was supported in part by the National Natural Science Foundation of China under Grant 61971384 and Grant 62071436.

REFERENCES

[1] S. M. Radha, M. Jung, P. Park, and I.-J. Yoon, "Design of an electrically small planar quasi-isotropic antenna for enhancement of wireless link reliability under NLOS channels," *Appl. Sci.*, vol. 10, no. 18, paper 6204, Sep. 2020.

[2] J. Kim, J. Park, A. A. Omar, and W. Hong, "A symmetrically stacked planar antenna concept exhibiting

quasi-isotropic radiation coverage," *IEEE Antennas Wireless Propag. Lett.*, vol. 19, no. 8, pp. 1390-1394, Aug. 2020.

[3] P. F. Hu, Y. M. Pan, X. Y. Zhang, and B. J. Hu, "A compact quasi-isotropic dielectric resonator antenna with filtering response," *IEEE Trans. Antennas Propag.*, vol. 67, no. 2, pp. 1294-1299, Feb. 2019.

[4] S. I. Hussain Shah, S. M. Radha, P. Park, and I.-J. Yoon, "Recent advancements in quasi-isotropic antennas: A review," *IEEE Access*, vol. 9, pp. 146296-146317, 2021.

[5] J. Ouyang, Y. M. Pan, S. Y. Zheng, and P. F. Hu, "An electrically small planar quasi-isotropic antenna," *IEEE Antennas Wireless Propag. Lett.*, vol. 17, no. 2, pp. 303-306, Feb. 2018.

[6] Q. Li, W.-J. Lu, S.-G. Wang, and L. Zhu, "Planar quasi-isotropic magnetic dipole antenna using fractional-order circular sector cavity resonant mode," *IEEE Access*, vol. 5, pp. 8515-8525, 2017.

[7] S. M. Radha, G. Shin, P. Park, and I.-J. Yoon, "Realization of electrically small low-profile quasi-isotropic antenna using 3D printing technology," *IEEE Access*, vol. 8, pp. 27067-27073, 2020.

[8] Y. Wang, M.-C. Tang, D. Li, K.-Z. Hu, M. Li, and X. Tan, "Low cost electrically small quasi-isotropic antenna based on split ring resonator," *Proc. Int. Appl. Comput. Electromagn. Soc. Symp.-China (ACES)*, pp. 1-2, Aug. 2019.

[9] S. Li, *System and Methodology of Look Ahead and Look Around LWD Tool*: U.S. Patent 10,605,073, 2020-3-31.

[10] R. F. Harrington, *Field Computation by Moment Methods*, MacMillan, New York, 1968.

[11] X. X. Nie, H. L. Liu, J. B. Liu, and J. M. Song, "Research on the small circular arc antenna based on the method of moments," *2022 International Applied Computational Electromagnetics Society (ACES-China) Symposium*, 2022.

[12] L. Li, L. C. Wang, X. L. Yin, and S. F. Li, "Design of an electrically small and near-3D omnidirectional loop antenna for UHF band RFID tag," 2013 *IEEE International Conference on Microwave Technology & Computational Electromagnetics*, pp. 246-248, 2013.

[13] C. A. Balanis, *Antenna Theory: Analysis and Design*, John Wiley & Sons, New York, 2015.

[14] W. L. Stutzman and G. A. Thiele, *Antenna Theory and Design*, John Wiley & Sons, New York, 2012.

[15] J. G. Van Bladel, *Electromagnetic Fields*, John Wiley & Sons, New York, 2007.

[16] J. M. Jin, *Theory and Computation of Electromagnetic Fields*, John Wiley & Sons, New York, 2010.

[17] CST Microwave Studio, ver. 2020, Computer Simulation Technology, Framingham, MA, 2020.

Hailong Liu received the B.S. degree in communication engineering and the M.S. degree in electronic information from Communication University of China, Beijing, China, in 2019 and 2023, respectively.

His research interests include computational electromagnetics and antenna design for RFID tags.

Jinbo Liu received the B.S. degree in electronic information engineering from Zhengzhou University, Zhengzhou, China, in 2010, and the Ph.D. degree in electronic science and technology from Beijing Institute of Technology, Beijing, China, in 2016.

He is currently an associate professor with the School of Information and Communication Engineering, Communication University of China, Beijing. His current research interests include computational electromagnetics and its applications, and frequency selective surfaces design.

Xiaoxia Nie received the B.S. degree in electronic information engineering from Taiyuan University of Technology, Taiyuan, China, in 2019, and the M.S. degree in electronic information from Communication University of China, Beijing, China, in 2022.

Her research interests include computational electromagnetics and antenna theory and design.

Jiming Song received the Ph.D. degree in electrical engineering from Michigan State University in 1993. From 1993 to 2000, he worked as a postdoctoral research associate, a research scientist and visiting assistant professor at the University of Illinois at Urbana-Champaign. From 1996 to 2000, he worked part-time as a research scientist at SAIC-DEMACO. Dr. Song was the principal author of the Fast Illinois Solver Code (FISC). He was a principal staff engineer/scientist at Semiconductor Products Sector of Motorola in Tempe, Arizona, before he joined the Department of Electrical and Computer Engineering at Iowa State University as an assistant professor in 2002.

Dr. Song currently is a professor at Iowa State University's Department of Electrical and Computer Engineering. His research has dealt with modeling and simulations of electromagnetic, acoustic and elastic wave propagation, scattering, and non-destructive evaluation, electromagnetic wave propagation in metamaterials and periodic structures and applications, interconnects on lossy silicon and radio frequency components, antenna radiation and electromagnetic wave scattering using fast algorithms, and transient electromagnetic fields. He received the NSF Career Award in 2006 and is an IEEE Fellow and ACES Fellow.

Zengrui Li received the B.S. degree in communication and information system from Beijing Jiaotong University, Beijing, China, in 1984, the M.S. degree in electrical engineering from Beijing Broadcast Institute, Beijing, China, in 1987, and the Ph.D. degree in electrical engineering from Beijing Jiaotong University, Beijing, China, in 2009.

He is currently a professor with the School of Information and Communication Engineering, Communication University of China, Beijing, China. He was a visiting scholar at Yokohama National University, Yokohama, Japan, from 2004 to January 2005. He also served as a senior visiting fellow at Pennsylvania State University from October 2010 to January 2011. His research interests include the areas of finite-difference time-domain (FDTD) methods, electromagnetic scattering, metamaterials and antennas. He is a senior member of the Chinese Institute of Electronics.